

# Upregulation of long noncoding RNA MALAT1 in colorectal cancer promotes radioresistance and malignance

Wenqi Shen

Second Affiliated Hospital of Soochow University

Qifeng Yu

Second Affiliated Hospital of Soochow University

Yuwei Pu

Second Affiliated Hospital of Soochow University

Chungen Xing (✉ [Xingcg@suda.edu.cn](mailto:Xingcg@suda.edu.cn))

Second Affiliated Hospital of Soochow University

---

## Research Article

**Keywords:** lnc RNA MALAT1, radiation sensitivity, aggressive phenotypes, colorectal cancer, prognosis

**Posted Date:** April 15th, 2022

**DOI:** <https://doi.org/10.21203/rs.3.rs-1532100/v1>

**License:**  This work is licensed under a Creative Commons Attribution 4.0 International License.

[Read Full License](#)

---

# Abstract

**Background:** Metastasis-associated lung adenocarcinoma transcript 1 (MALAT1), a conserved transcript with 8,000 nt, is highly associated with malignancy of numerous cancer types. However, the function of MALAT1 plays in regulating the response to radiotherapy in colorectal cancer (CRC) remains unclear. Thus, the object of this study is to investigate the functions of MALAT1 in CRC radioresistance.

**Methods:** First, the expression of MALAT1 in colon adenocarcinoma (COAD) was analyzed through the Cancer Genome Atlas (TCGA) database. Then, we detected the expression level of MALAT1 in tumor tissues and CRC cell lines and analyzed the relevance of MALAT1 and clinicopathological parameters. In the end, the effect of silencing MALAT1 on the radiosensitivity of CRC cells was investigated, and its potential mechanism was preliminarily illustrated.

**Results:** The analysis of TCGA data showed that MALAT1 was closely related to the type of tumor, and high expression of MALAT1 was remarkably relevant to poor outcome. MALAT1 was highly expressed in CRC tissues and cell lines and related to tumor stages. Knockdown of MALAT1 could significantly suppress colony survival, proliferation, and migration and increase apoptosis, G2/M phase arrest, and formation of gamma-H2AX foci in HCT116, whether in combination with X-rays or not. Moreover, Kyoto Encyclopedia of Genes and Genomes (KEGG) pathway analysis demonstrated that the regulated proteins were principally enriched in the glycosaminoglycan degradation pathway after silencing MALAT1.

**Conclusion:** Our results implied that MALAT1 was highly expressed in CRC and associated with tumor stage and prognosis. Silencing MALAT1 can increase HCT116 cell radiosensitivity, which may be potentially influenced by glycosaminoglycan degradation pathway.

## Background

Colorectal cancer (CRC) has become one of the most frequent malignant tumors and the second-leading cause of tumor-related deaths with poor prognosis[1]. Routine treatment strategies include surgical resection, radiotherapy (RT), and chemotherapy[2]. Although therapeutic schedules have modified significantly over the years, the survival rate and prognosis of CRC patients are still unfavorable. Radiotherapy is an important treatment for advanced and metastatic cancers, however, the occurrence of radioresistance limits the usage of RT in clinical treatments[3]. In spite of the many studies that have been conducted on CRC, the underlying mechanism remains unclear. Therefore, finding a potential target and improving radiosensitivity may play a critical role in CRC treatment.

Long noncoding RNAs, with transcripts 200 to 100,000 nucleotides (nt) in length, have no ability to code proteins but participate in the regulation of gene expression and protein synthesis[4]. Metastasis-associated lung adenocarcinoma transcript 1 (MALAT1), one of conserved long noncoding RNA and highly abundant in normal tissues, has been reported to participate in numerous cancers[5]. High expression of MALAT1 was relevant to poor prognosis of CRC[6]. MALAT1 was associated with malignancy of CRC by promoting CRC cell proliferation, migration, and invasion through different

mechanisms[7–9]. At the same time, a high level of MALAT1 in CRC was associated with chemoresistance, and downregulated MALAT1 could improve the response to chemotherapy in CRC patients[10, 11]. MALAT1 was also reported to participate in modulating radiosensitivity of cervical cancer[12] and affect the response to radiotherapy of esophageal squamous cell carcinoma through regulating Cks1 expression as well[13]. However, few studies have focused on the relationship between MALAT1 and radiosensitivity of CRC, and the underlying mechanism is still unclear and requires more attention. In this work, we confirmed that MALAT1 was highly expressed in both tumor tissues and CRC cell lines. Silencing of MALAT1 in CRC cells significantly increased the radiosensitivity. Finally, we preliminarily investigated the potential mechanism for MALAT1 improving CRC radiosensitivity.

## Methods

### Study population

For clinical parameter analysis, we collected 57 groups of primary CRC samples and adjoining noncancerous colorectal specimens from CRC patients who experienced radical operation without or radiotherapy or chemotherapy at the Second Affiliated Hospital of Soochow University (Soochow, China) from 2013 to 2015. All tissues were immediately frozen in centrifuge tubes containing RNAlater preservation liquid after excision and preserved in  $-80^{\circ}\text{C}$  until RNA extraction. Informed consents from the whole patients were obtained, and this research was approved by the Ethics Committee of Soochow University.

### Cell culture and transfection

A human intestinal epithelial cell line (HIEC) and CRC cell lines (SW480, HCT8, HT29, HCT116, RKO, colo205 and Lovo) were purchased from Shanghai Chinese Academy of Sciences (Shanghai, China). Cells were cultured in DMEM (HyClone, Logan, UT, USA) containing 10% fetal bovine serum (FBS; HyClone) and 1% Penicillin–Streptomycin solution (Beyotime, Shanghai, China) at  $37^{\circ}\text{C}$  in a humidified atmosphere with 5%  $\text{CO}_2$ . The studies were carried out when the cells reached 70–80% confluence. HCT116 cell was seeded into 48-well plates and transfected with lentivirus-mediated control shRNA or lentivirus-mediated shRNA targeting LncRNA-MALAT1, designated shNC and shLncRNA-MALAT1, respectively. The lentivirus-mediated shRNA was purchased from Hanbio Biotechnology (Shanghai, China). The cells were subsequently harvested at 48 h post transfection and selected in puromycin at a dose of  $3\ \mu\text{g}/\text{mL}$  (Sigma-Aldrich, St. Louis, MO, USA). The stably transfected cell lines were validated by real-time PCR and then used for the subsequent experiments. Sequences of shRNA were shown in supplementary table S1.

### Cell proliferation assay

Cell proliferation was tested by the Cell Counting Kit 8 (Beyotime Biotechnology, China). The stably transfected cell lines HCT116-shLnc RNA-MALAT1 and HCT116-shNC were respectively seeded in 96-well plates ( $4 \times 10^3$  cells/well). Then, 100  $\mu\text{L}$  of DMEM containing 10% CCK8 reagent was added to each well

after 24 h, 48 h, 72 h, and 96 h and cultured for an additional 2 h. The absorbance of each well was measured by a microplate reader (Bio-Rad, Hercules, CA, USA) at a wavelength of 450 nm. Three independent experiments were performed.

## **RNA extraction and quantitative real-time PCR**

Total RNA was obtained using TRIzol reagent (Invitrogen, Carlsbad, CA, USA) from the stably transfected cells, and total RNA (1 µg) was reverse transcribed to cDNA using 5× All-In-One RT MasterMix (abm, ZhenJiang, China). Quantitative real-time PCR was completed using SYBR-Green Mix and detected by the AB ViiA7 Sequence Detection System (Applied Biosystems, Foster City, CA, USA). The mRNA level of LncRNA-MALAT1 was detected by quantitative real-time PCR, and GAPDH was used as an endogenous standard to normalize the expression of LncRNA-MALAT1. The primer pairs were shown in supplementary table S1.

## **Western blot assay**

For western blotting assay, the stably transfected cells were put into 6-well plates and collected after 24 h and then lysed using cell lysis buffer. The concentration of total protein was measured using a BCA Protein Assay Kit (Beyotime Biotechnology, China). Then, proteins were isolated by SDS-PAGE and transferred to PVDF membranes. Following primary antibodies were used for western blot analysis: MMP2, Vimentin, γ-H2AX, Bcl-2, E-cadherin, and Bax (1:1000, Abcam, Cambridge, USA); and GAPDH (1:2000, Beyotime Biotechnology, China) was used as an internal control.

## **Colony formation assay**

Stably transfected cells were seeded into 6-well plates at 300–5,000 cells/well after resuspending and cultured for 24 h, and then the cells were exposed to 0, 2, 4, 6, and 8 Gy X-ray at a dose rate of 1.15 Gy/min using a linear accelerators. After another 10 to 14 days' incubation, the cells were fixed using 4% paraformaldehyde for 30 minutes, and dyed with a crystal violet solution. The colonies including at least 50 cells were counted. A multitarget single-hit model was used for the measure of radiation sensitivity enhancement ratio (SER).

## **Cell apoptosis assay**

Transfected cells were put into 6-well plates and then exposed to 4 Gy X-ray irradiation. The cells were collected after 48 h incubation and stained with Annexin V-PE and 7-AAD (BD Biosciences, NJ, USA). Apoptotic cells were determined by flow cytometry (BD Biosciences, NJ, USA).

## **Cell cycle progression analysis**

Cells were fixed using 70% cold ethanol overnight after irradiation and then stained by propidium iodide (Sigma-Aldrich, St. Louis, MO, USA) for an additional 30 min at 37°C before detection. The portion of the population in each phase of cell cycle was detected using flow cytometry (BD Biosciences, NJ, USA).

## **Wound healing migration assay**

To detect the wound healing migration, cells were seeded into 6-well plates and incubated for 24 h. After 4 Gy X-ray irradiation, the cells were scratched using a yellow pipette tip and washed three times with phosphate buffer saline (PBS). Then, cells were cultured with serum-free DMEM, and images were obtained using a microscope (Olympus, Tokyo, Japan) at 0 h and 72 h.

## Immunofluorescence

Cells were fixed with 4% paraformaldehyde for 30 min and washed three times with PBS. Then the cells were treated with 1% Triton X-100 for 10 min and then blocked with 5% bovine serum albumen for 1 hour. After washing with PBS, cells were incubated with specific primary anti-gamma H<sub>2</sub>AX antibodies (1:1000; Abcam) for 3 h at room temperature. Then the cells were incubated with Cy3-conjugated anti-mouse IgG (1:1000; Abcam) for 1 h away from light and then washed three times with PBS for 10 min/wash. Nuclei were stained with 4',6-diamidino-2-phenylindole (DAPI; Sigma-Aldrich, USA). Finally, cells were observed through a laser confocal microscope IX71 (Olympus, Tokyo, Japan) with a digital camera (Olympus, Tokyo, Japan), and then  $\gamma$ -H2AX foci were calculated in each cell. About 50 cells were counted in 10 randomly fields of view.

## iTRAQ proteomic analysis

We knocked down MALAT1 in HCT116 through RNAi and extracted total proteins for iTRAQ analysis. Next, we used an integrated method involving LC-MS/MS and TMT labeling to quantify the dynamic changes of the whole proteome in HCT116 siMALAT1 compared with siNC. Sequences of siRNA are shown in supplementary table S1.

## R-4.0.2

R is open-source software that can be used for statistical calculations and statistical mapping. We downloaded colorectal cancer expression profile and clinical information data from TCGA via UCSC (<http://xena.ucsc.edu/>). Gene Set Enrichment Analysis (GSEA) was used to evaluate the distribution trend of genes in a predefined gene set in the sequence of phenotypic relevance in order to determine their contribution to the phenotype. We used the GSEABase package to complete the enrichment analysis of the CRC expression profile. In addition, we carried out extensive cancer analysis of the enriched pathways in 33 cancers and explored the activation or inhibition status of the corresponding pathways in those cancers. The visualization of the final result was done by the ggplot2 package. Normalized enrichment score (NES) > 1.0 represents pathway activation and NES < - 1.0 represents pathway inhibition; a p-value < 0.05 was considered statistically significant.

## Statistical analysis

All of the experiments were performed at least three times. All results were showed using mean  $\pm$  standard error and analyzed using GraphPad Prism 8 software (San Diego, CA, USA). Student's t-test was employed to compare two groups. A p value of < 0.05 was considered as a statistically significant result (p-value markings: \*p < 0.05, \*\*p < 0.01 and \*\*\*p < 0.001).

# Results

## *LncRNA MALAT1 was highly expressed in CRC tissues and cell lines*

We compared MALAT1 expression levels between normal and cancer tissues via the Cancer Genome Atlas (TCGA) database. As it showed, MALAT1 was more elevated in tumor tissues compared to normal tissues in CRC (Fig. 1A). We divided CRC patients in TCGA database into MALAT1\_low and MALAT1\_high groups on the basis of the median MALAT1 expression value. The overall survival was shorter in the MALAT1\_high group than that in the MALAT1\_low group (Fig. 1B). To investigate the involvement of MALAT1 in CRC progression, we detected MALAT1 expression in both primary tumor and metastatic tumor tissues, and discovered that MALAT1 expression was significantly increased in the metastatic tumors (Fig. 1C). Real-time PCR assay was used to investigate the expression of MALAT1 in resected CRC tissues and corresponding adjacent normal tissues (n = 57). The results showed that MALAT1 expression was higher in CRC tissues comparing with that of non-tumor tissues (Fig. 1D–E). The clinicopathological characteristics of the registered patients were shown in Table 1. Then, we detected the expression of MALAT1 in a normal intestinal epithelial cell line, HIEC, and CRC cell lines including HCT116, SW480, HCT8, HT29, RKO, LOVO, and colo205. The results showed that HCT116 cell possessed the highest expression of MALAT1 (Fig. 1F). Therefore, HCT116 was chosen for subsequent designs to study the role of MALAT1 in CRC radiosensitivity.

Table 1  
The statistic of clinicopathological characteristics from 57 CRC patients

| <b>Clinical parameters</b>   | <b>Numbers</b> |
|------------------------------|----------------|
| Cases                        | 57             |
| <b>Age</b>                   |                |
| < 65                         | 32             |
| ≥ 65                         | 25             |
| <b>Tumor size</b>            |                |
| Small size (< 5 cm)          | 27             |
| Large size (≥ 5 cm)          | 30             |
| <b>Gender</b>                |                |
| Male                         | 37             |
| Female                       | 20             |
| <b>Invasion levels</b>       |                |
| Mucosa                       | 5              |
| Submucosa                    | 4              |
| Muscle                       | 10             |
| Serosa                       | 37             |
| <b>TNM stage</b>             |                |
| Stage 1–2                    | 36             |
| Stage 3–4                    | 21             |
| <b>Lymph node metastasis</b> |                |
| Positive                     | 28             |
| Negative                     | 29             |
| <b>Grade of tumors</b>       |                |
| Low grade                    | 15             |
| Intermediate grade           | 34             |
| High grade                   | 8              |
| <b>Vascular invasion</b>     |                |

| Clinical parameters        | Numbers |
|----------------------------|---------|
| Positive                   | 24      |
| Negative                   | 33      |
| <b>Perineural invasion</b> |         |
| Positive                   | 19      |
| Negative                   | 38      |

### ***Downregulated expression of MALAT1 inhibited the proliferation of HCT116***

Lentivirus-mediated shRNA targeting MALAT1 was used to knock down MALAT1 expression, and puromycin (3 ug/mL) was used to select stably transfected cells. The transfected efficiency was verified by real-time PCR (Fig. 2A). To confirm the short-term influence of MALAT1 silencing-related growth inhibition in human CRC HCT116, stably transfected cells were seeded and incubated for 24 h, 48 h, 72 h, and 96 h, and cell viability was measured by CCK8 assays. As shown in Fig. 2B, MALAT1 silencing inhibited the proliferation of HCT116. A long-term effect of proliferative inhibition was determined by colony formation assays, which implied that MALAT1 silencing remarkably decreased the number of colonies (Fig. 2C–D). These results suggested that MALAT1 silencing inhibited CRC cell proliferation.

### ***MALAT1 silencing inhibited migration in CRC cells***

Wound healing migration assays were performed to estimate the effect of MALAT1 on migration. The ability of cell migration was obviously suppressed due to MALAT1 silencing, and the inhibitory effect became more distinct after 4 Gy X-ray treatment (Fig. 3A–B). We tested the expression of metastasis-related proteins through western blotting assays. The results showed that the expression level of matrix metalloproteinase 2 (MMP2) and Vimentin were declined and E-cadherin was increased in HCT116 cells after transfecting with shRNA target MALAT1 (Fig. 3C), and such changes were more distinct in combination with irradiation. Taken together, we surmised that the downregulation of MALAT1 in HCT116 cells could significantly impair the migration of HCT116 cells.

### ***MALAT1 silencing enhanced the radiosensitivity of HCT116***

The plate clone formation assay was considered as the gold standard in evaluating radiosensitivity. Cells stably transfected with shRNA targeted MALAT1 and NC were seeded into 6-well plates in different densities, then exposed to 0, 2, 4, 6, and 8 Gy X-rays respectively and incubated for another 10 days. A multitarget single-hit model was used to explore the effect of MALAT1 silencing on radiosensitivity of HCT116 cells. After MALAT1 silencing, the radiosensitivity of HCT116 was improved as shown in Fig. 4A. D0 values were used to appraise the radiosensitivity, and higher D0 values indicated lower sensitivity to radiation. The results showed that MALAT1 silencing could remarkably decline the levels of colony formation after irradiation, and the downregulation of MALAT1 (D0 sh1 = 0.8122, D0 sh3 = 0.8010) significantly reduced the colony survival fraction in a dose-dependent manner, compared with the NC

group (D0 = 0.8882) (Fig. 4B and Table 2). According to the parameters of radiosensitization showed in Table 2, downregulating MALAT1 in HCT116 exhibited higher sensitivity enhancement ratios (SER) (SER sh1 = 1.0936, SER sh3 = 1.1089). Thus, the results showed that silencing MALAT1 could increase the radiosensitivity of CRC cells.

### ***Knockdown of MALAT1 induced cell cycle arrest***

In addition to the results from prior experiments, we used TCGA data to conduct a generalized analysis of the G2/M checkpoint and found that the G2/M checkpoint was significantly activated in CRC (Fig. 4C). Although there was no correlation between the G2/M checkpoint and MALAT1 (Fig. 4D–E), the following results confirm that downregulation of MALAT1 combined with 4 Gy X-ray irradiation could lead to more G2/M phase arrest in HCT116 cells (Fig. 4F–G). These data indicated that MALAT1 silencing combined with X-rays could increase the radiosensitivity of CRC cells via activating the G2/M checkpoint.

Table 2  
The D0, Dq, N and SER values in NC, sh-MALAT1 and sh-MALAT3 transfected HCT116 cells. The SER value was artificial using the multi-target single hit model.

| Group       | D0     | Dq     | N     | SER    |
|-------------|--------|--------|-------|--------|
| NC          | 0.882  | 1.727  | 6.991 |        |
| Sh-MALAT1-1 | 0.8122 | 1.0412 | 3.604 | 1.0936 |
| Sh-MALAT1-3 | 0.801  | 1.1862 | 4.397 | 1.1089 |

### ***MALAT1 silencing induced DNA double-strand breaks in CRC cells***

Thereafter, a generalized analysis of the DNA\_REPAIR found that DNA\_REPAIR was significantly activated in CRC (Fig. 5A–B). In addition, there was a significant positive correlation between DNA\_REPAIR and MALAT1 expression (Fig. 5C). To examine whether MALAT1 silencing improved the formation of nuclear  $\gamma$ -H2AX foci induced by irradiation at 0, 0.5, 4, and 12 h, western blot analysis was conducted (Fig. 5D). The results confirmed that MALAT1 silencing could significantly increase the formation of  $\gamma$ -H2AX foci after 4 Gy X-ray irradiation, especially at 0.5 h, which was further confirmed by immunofluorescence assay (Fig. 5E–F). These results suggested that MALAT1 silencing could induce higher expression of  $\gamma$ -H2AX and more  $\gamma$ -H2AX foci formation, regardless of whether it is combined with irradiation.

### ***MALAT1 silencing induced apoptosis in CRC cells***

Severe DNA damage may result in apoptosis, so we further investigated the relationship between apoptosis and the expression of MALAT1. As shown in Fig. 6A–B, apoptosis was significantly inhibited in CRC. Moreover, the expression level of MALAT1 was negatively relevant to apoptosis (Fig. 6C). Then, we verified the impact of MALAT1 on CRC cells using flow cytometry analysis. The results demonstrated that MALAT1 silencing increased apoptosis, and it was more obvious after combining it with radiotherapy (Fig. 6D). As showed in Fig. 6E, the apoptotic ratios of shMALAT1-1 ( $6.77 \pm 0.31\%$ ) and shMALAT1-3

( $6.71 \pm 0.26\%$ ) were significantly higher than that of shNC ( $3.33 \pm 0.17\%$ ). After 4 Gy X-ray irradiation, the apoptotic ratios came to  $20.15 \pm 1.38\%$  in shMALAT1-1,  $24.16 \pm 1.85\%$  in shMALAT1-3 and  $6.32 \pm 0.63\%$  in shNC. However, we detected the expression of apoptosis-related proteins. The expression of BAX was increased, and Bcl-2 was decreased after cells were treated with shRNA targeted MALAT1 compared to NC, especially when it was combined with radiotherapy (Fig. 6F). All of these results suggested that MALAT1 silencing could increase apoptosis in CRC cells.

### ***Preliminary proteomic analysis indicated the underlying mechanisms of MALAT1 in CRC***

To investigate the difference of protein levels between HCT116 siMALAT1 and HCT116 siNC, we extracted total proteins of stably transfected cells and then conducted iTRAQ proteomic analysis. The amounts of the total identified and quantified proteins as well as differentially expressed proteins are separately summarized in Supplemental Table S2-3. Twenty-seven proteins (quantitative ratio over 1.3) were found to be upregulated, whereas 46 proteins (quantitative ratio less than 0.77) were downregulated. Volcano plot displayed the top 10 up- and downregulated proteins in HCT116 siMALAT1 compared with HCT116 siNC (Fig. 7A and Table S4-5); the green ball represented downregulated proteins and the red ball represented upregulated ones. To further analyze their functions, the differentially-abundant proteins (DAPs) were categorized into the major Gene Ontology (GO) categories—biological process (BP), cellular component (CC), and molecular function (MF)—based on their GO annotations. The mainly enriched proteins in BP were related with the following terms: protein maturation by protein folding, regulation of protein depolymerization, regulation of protein complex disassembly, ensheathment of neurons, and protein maturation (Fig. 7B). In the CC category, the predominantly enriched terms were elongin complex, Flemming body, F-actin capping protein complex, dynactin complex, and microtubule associated complex (Fig. 7C). The DAPs in the MF category were connected with the following terms: complement component C1q binding, protein complex binding, macromolecular complex binding, complement binding, and opsonin binding (Fig. 7D). The detailed results of GO enrichment analysis are given in Supplemental Table S6-8. To further investigate the discrepancy between the cellular pathways of HCT116 siMALAT1 and HCT116 siNC, KEGG enrichment analysis was performed via DAVID. The results indicated that the whole DAPs mapped to 34 KEGG pathways. The pathways of the DAPs based on the KEGG database are shown in Fig. 7E. The maximal number of DAPs were enriched in the glycosaminoglycan degradation, human immunodeficiency virus 1 infection, Ubiquitin-mediated proteolysis, glycosphingolipid biosynthesis-globo and isoglobo series, and lysosome pathways, detailed results of which can be found in Supplemental Table S9. These signaling pathways may play an crucial role in MALAT1 silencing HCT116, and more research ought to be carried out on them.

## **Discussion**

The recent treatments for CRC include surgery, chemotherapy and radiotherapy. Radiotherapy is the basis of clinical strategy for CRC patients. However, radioresistance is a crucial challenge in the usage of radiotherapy in clinical practice, so identifying the underlying mechanisms associated with radioresistance is urgently needed. Radioresistance is considered to be related to multiple elements,

including microenvironmental hypoxia[14], activation of DNA repair[15, 16], autophagy induced by radiotherapy or hypoxia[17, 18], aberrant pathway activation such as PI3K/AKT[19, 20], and many other classical processes. Recently, the relationships between lncRNA and cancer resistance have been frequently reported. Most researchers have found that lncRNA participates in regulating the effects of various cancer therapies. Long noncoding RNA MALAT1 is highly expressed in numerous cancers, including lung cancer[21], CRC[6], bladder cancer[22], etc., and its abundance and aberrant expression make it vital to the development of cancer. It has been reported that high expression of MALAT1 is closely related with poor prognosis[23, 24], growth[25, 26], metastasis[27] and chemoresistance[28–30]. Recently, MALAT1 has been found to participate in regulating tumor radioresistance. Yuan et al. [31] reported that DNA damage induced by radiotherapy would upregulate MALAT1 and then result in undesirable inflammation. Guo et al. [32] found that MALAT1 modulated radioresistance in CRC via miR-101-3p sponge. Up to this point, we have investigated the role of MALAT1 in CRC radiotherapy. Previous studies have confirmed that MALAT1 was highly expressed and associated with malignancy in various cancers[33–35], which was consistent with our findings. Therefore, we propose that MALAT1 may be a potential target in radiotherapy of CRC. In this study, MALAT1 was found to be overexpressed in CRC and was associated with tumor malignancy and radiosensitivity. We discovered that MALAT1 was highly expressed in both CRC cell lines and tissues and was closely correlated with tumor stages and survival, which suggested that MALAT1 plays an important role in the development of CRC. In order to explore the functions of MALAT1, we knocked down the expression of MALAT1 in HCT116 using lentivirus-mediated shRNA and detected the efficiency of transfection by RT-PCR. MALAT1 was reported to promote growth in multiple cancers[7, 25, 36, 37], which was further confirmed in our study. CCK8 and colony formation assays showed that silencing MALAT1 inhibited both short- and long-term proliferation of HCT116. Epithelial-mesenchymal transition (EMT) is a representative progress in tumor aggressive phenotypes. So, we investigated the migration ability via wound healing migration assay and relative protein expressions. As expected, silencing MALAT1 inhibited the migration of HCT116, and this effect was more prominent when combined with radiation therapy. In addition, western blotting assays confirmed that silencing MALAT1 together with radiotherapy invited a significant upregulation of E-cadherin and downregulation of MMP2 and Vimentin, which indicated the inhibition of EMT in HCT116 and then further influenced the migration. MALAT1 silencing would obviously increase the radiosensitivity of HCT116 according to our results. Histone gamma-H2AX foci would be formed after DNA double-strand breaks induced by IR, and the rate of disappearance of  $\gamma$ -H2AX after irradiation was related to the radiosensitivity of cells[38]. Gong et al. [39] demonstrated that quercetin suppressed DNA double-strand break repair and enhanced the radiosensitivity of human ovarian cancer cells via the p53-dependent endoplasmic reticulum stress pathway. In this study, immunofluorescence and western blot assay both demonstrated that knockdown of MALAT1 could induce more gamma-H2AX foci formation in HCT116 after 4 Gy X-ray irradiation compared with NC and delay the disappearance at the same time, which suggested that knocking down MALAT1 in HCT116 would inhibit the progress of DNA damage repair and induce more cell deaths. Modulation of radiosensitivity may arise from G2/M checkpoint activation[40]. It was reported that G2/M phase arrest and apoptosis induced by celecoxib enhanced radiosensitivity in nasopharyngeal carcinoma[41]. So, we detected the cell cycle and apoptosis to further study the

functions of MALAT1 on HCT116. We found that silencing MALAT1 had no influence on the cell cycle compared with the control group, which was in accordance with the results from our experiment in which MALAT1 was unrelated to the G2/M checkpoint pathway. But downregulation of MALAT1 could obviously lead to more cells undergoing G2/M phase arrest in combination with X-rays, which may be in accord with the results from our experiment in which MALAT1 could activate the G2/M checkpoint and then increase the radiosensitivity of HCT116. At the same time, the apoptosis rate was higher after knockdown of MALAT1 in HCT116, and related proteins associated with apoptosis, including BAX and Bcl-2, showed a consistent trend suggesting that knocking down of MALAT1 would affect the expression levels of apoptosis-related proteins. Moreover, we preliminarily investigated the potential mechanism through iTRAQ proteomic analysis. Through the volcano plot, 46 proteins (quantitative ratio less than 0.77) were downregulated in HCT116 siMALAT1, including ankyrin repeat and KH domain containing 1 (ANKHD1). ANKHD1 was highly expressed in multiple cancer tissues and participated in cancer progression, including proliferation and invasion. Researchers have found that knocking down ANKHD1 in HCT116 could reduce tumor malignancy[42]. It may explain the functions of MALAT1 exhibiting in HCT116, but the detailed mechanism between ANKHD1 and MALAT1 has not yet been thoroughly investigated. Moreover, KEGG pathway enrichment analysis revealed that upregulated proteins were mainly enriched in the glycosaminoglycan degradation pathway. Glycosaminoglycans (GAGs) are expressed on almost all mammalian cells and play an important role in various physiological and pathological processes, such as tumor growth, inflammation, bacterial and viral infections, and Alzheimer's disease[43]. Given its role in multiple diseases, GAG has been used in the development of drugs, many of which have achieved encouraging results in animal models and clinical trials. Researchers developed one GAG modification drug by binding malaria protein with GAG to target human cancers[44]. GAGs are related with cancer growth, progression, and metastasis through interacting with growth factors, growth factor receptors, and cytokines[45]. Decreasing malignancy of HCT116 in silencing MALAT1 may be associated with the activation of the GAG degradation pathway. Of course, the underlying mechanisms of MALAT1-enhanced radiosensitivity need to be studied further. Overall, our data suggested that MALAT1 might serve as a promising therapeutic target for CRC patients with radioresistance.

## Conclusions

In summary, we found that MALAT1 was highly expressed in CRC tissues and cell lines. Downregulated MALAT1 enhanced radiosensitivity of HCT116 by inducing apoptosis, G2/M phase arrest, DNA double-strand breaks, and synergic inhibition of aggressive phenotypes. The iTRAQ proteomic analysis revealed that the glycosaminoglycan degradation pathway may play a crucial role in the high expression of MALAT1 leading to cancer radioresistance. Although the underlying mechanisms by which MALAT1 regulates the radiosensitivity of CRC cells need to be studied further, our findings suggested that MALAT1 may be a potential therapeutic target in the radiotherapy of CRC.

## Abbreviations

| Abbreviations | Full name                                                                |
|---------------|--------------------------------------------------------------------------|
| Lnc-MALAT1    | Long nocoding RNA-Metastasis-associated lung adenocarcinoma transcript 1 |
| CRC           | Colorectal cancer                                                        |
| COAD          | colon adenocarcinoma                                                     |
| TCGA          | the Cancer Genome Atlas                                                  |
| KEGG          | Kyoto Encyclopedia of Genes and Genomes                                  |
| PBS           | phosphate buffer saline                                                  |
| DAPI          | 4',6-diamidino-2-phenylindole                                            |
| MMP2          | matrix metalloproteinase 2                                               |
| DAPs          | differentially-abundant proteins                                         |
| GO            | Gene Ontology                                                            |
| BP            | biological process                                                       |
| CC            | cellular component                                                       |
| MF            | molecular function                                                       |
| ANKHD1        | ankyrin repeat and KH domain containing 1                                |
| GAGs          | Glycosaminoglycans                                                       |

## Declarations

### Ethics approval and consent to participate

Written informed consent had been obtained from all the participants, and this research was approved by the Ethics Committee of Soochow University. I confirmed that research methods involving human material were performed in accordance with the Declaration of Helsinki and all other methods were performed in accordance with the relevant guidelines and regulations.

### Consent for publication

Not applicable.

### Availability of data and materials

The original contributions presented in the study are accessible in the supplementary material. Further requiries can connect the corresponding authors.

### Competing interests

The authors declare that they have no competing interests

## Funding

This work was financially supported by the Health and Family Planning Commission Fund Project of Jiangsu Province (No. CXTDA2017016), State Key Laboratory of Radiation Medicine and Protection, Soochow University (GZK1202010), and the National Natural Science Foundation of China (81672970).

## Authors' contributions

WS completed the main experiments, and writing; QY completed the bioinformatics analysis and writing. CX and YP completed the design and guidance of the subject, and made major revisions to the manuscript. All authors contributed to the article and approved the submitted version.

## Acknowledgements

Not applicable

## References

1. F. Bray, J. Ferlay, I. Soerjomataram, R. Siegel, L. Torre, A. Jemal, Erratum: Global cancer statistics 2018: GLOBOCAN estimates of incidence and mortality worldwide for 36 cancers in 185 countries. *CA Cancer J Clin* (2020) 70:313. doi: 10.3322/caac.21609.
2. F.H.W. Jonker, P.J. Tanis, P.-P.L.O. Coene, E. van der Harst, o.b.o.t.D.S.C.A. Group, Impact of Neoadjuvant Radiotherapy on Complications After Hartmann Procedure for Rectal Cancer. *Dis Colon Rectum* (2015) 58:931–937. doi: 10.1097/DCR.0000000000000432.
3. F. Hosseini, M.R. Sam, N. Jabbari, H. Mozdarani, Modulating Survivin as a Radioresistant Factor, Caspase-3, and Apoptosis by Omega-3 Docosahexaenoic Acid Sensitizes Mutant-p53 Colorectal Cancer Cells to  $\gamma$ -Irradiation. *Cancer biotherapy radiopharmaceuticals* (2018) 33:387–395. doi: 10.1089/cbr.2018.2445..
4. J.L. Rinn, H.Y. Chang, Genome regulation by long noncoding RNAs. *Annual review of biochemistry* 81:145–166. doi:10.1146/annurev-biochem-051410-092902..
5. B. Zhang, G. Arun, Y.S. Mao, Z. Lazar, G. Hung, G. Bhattacharjee, X. Xiao, C.J. Booth, J. Wu, C. Zhang, The lncRNA Malat1 is dispensable for mouse development but its transcription plays a cis-regulatory role in the adult. *Cell reports* 2:111–123. doi: 10.1016/j.celrep.2012.06.003.
6. H.-T. Zheng, D.-B. Shi, Y.-W. Wang, X.-X. Li, Y. Xu, P. Tripathi, W.-L. Gu, G.-X. Cai, S.-J. Cai, High expression of lncRNA MALAT1 suggests a biomarker of poor prognosis in colorectal cancer. *International journal of clinical experimental pathology* 7:3174.
7. M.-H. Yang, Z.-Y. Hu, C. Xu, L.-Y. Xie, X.-Y. Wang, S.-Y. Chen, Z.-G. Li, MALAT1 promotes colorectal cancer cell proliferation/migration/invasion via PRKA kinase anchor protein 9. *Biochimica et Biophysica Acta -Molecular Basis of Disease* 1852:166–174. doi: 10.1016/j.bbadis.2014.11.013.

8. S. Wu, H. Sun, Y. Wang, X. Yang, Q. Meng, H. Yang, H. Zhu, W. Tang, X. Li, M. Aschner, MALAT1 rs664589 polymorphism inhibits binding to miR-194-5p, contributing to colorectal cancer risk, growth, and metastasis. *Cancer research* 79:5432–5441. doi: 10.1158/0008-5472.CAN-19-0773.
9. Q. Ji, L. Zhang, X. Liu, L. Zhou, W. Wang, Z. Han, H. Sui, Y. Tang, Y. Wang, N. Liu, Long non-coding RNA MALAT1 promotes tumour growth and metastasis in colorectal cancer through binding to SFPQ and releasing oncogene PTBP2 from SFPQ/PTBP2 complex. *British journal of cancer* (2014) 111:736–748. doi: 10.1038/bjc.2014.383.
10. P. Li, X. Zhang, H. Wang, L. Wang, T. Liu, L. Du, Y. Yang, C. Wang, MALAT1 is associated with poor response to oxaliplatin-based chemotherapy in colorectal cancer patients and promotes chemoresistance through EZH2. *Molecular cancer therapeutics* (2017) 16:739–751. doi: 10.1158/1535-7163.MCT-16-0591.
11. W. Chen, W. Zhao, L. Zhang, L. Wang, J. Wang, Z. Wan, Y. Hong, L. Yu, MALAT1-miR-101-SOX9 feedback loop modulates the chemo-resistance of lung cancer cell to DDP via Wnt signaling pathway. *Oncotarget* (2017) 8:94317. doi: 10.18632/oncotarget.21693..
12. H. Lu, Y. He, L. Lin, Z. Qi, L. Ma, L. Li, Y. Su, Long non-coding RNA MALAT1 modulates radiosensitivity of HR-HPV + cervical cancer via sponging miR-145. *Tumour Biology the Journal of the International Society for Oncodevelopmental Biology & Medicine* (2016) 37:1683. doi: 10.1007/s13277-015-3946-5.
13. Z. Li, Y. Zhou, B. Tu, Y. Bu, A. Liu, J. Kong, Long noncoding RNA MALAT1 affects the efficacy of radiotherapy for esophageal squamous cell carcinoma by regulating Cks1 expression. *Journal of Oral Pathology & Medicine* (2017) 46:583–590. doi: 10.1111/jop.12538.
14. D. Hennessey, L.M. Martin, A. Atzberger, T.H. Lynch, D. Hollywood, L. Marignol, Exposure to hypoxia following irradiation increases radioresistance in prostate cancer cells, *Urologic Oncology: Seminars and Original Investigations*, Elsevier, 2013, pp. 1106–1116.
15. A. Schulz, F. Meyer, A. Dubrovskaya, K. Borgmann, Cancer stem cells and radioresistance: DNA repair and beyond. *Cancers* (2019) 11:862. doi: 10.3390/cancers11060862..
16. A. Desai, B. Webb, S.L. Gerson, CD133 + cells contribute to radioresistance via altered regulation of DNA repair genes in human lung cancer cells. *Radiotherapy* 110:538–545. doi: 10.1016/j.radonc.2013.10.040..
17. S.L. Lomonaco, S. Finniss, C. Xiang, A. DeCarvalho, F. Umansky, S.N. Kalkanis, T. Mikkelsen, C. Brodie, The induction of autophagy by  $\gamma$ -radiation contributes to the radioresistance of glioma stem cells. *International journal of cancer* (2009) 125:717–722. doi: 10.1002/ijc.24402..
18. H. Feng, J. Wang, W. Chen, B. Shan, Y. Guo, J. Xu, L. Wang, P. Guo, Y. Zhang, Hypoxia-induced autophagy as an additional mechanism in human osteosarcoma radioresistance. *Journal of bone oncology* (2016) 5:67–73. doi: 10.1016/j.jbo.2016.03.001..
19. J. Bussink, A.J. van der Kogel, J.H. Kaanders, Activation of the PI3-K/AKT pathway and implications for radioresistance mechanisms in head and neck cancer. *The lancet oncology* (2008) 9:288–296. doi: 10.1016/S1470-2045(08)70073-1..

20. L. Chang, P.H. Graham, J. Ni, J. Hao, J. Bucci, P.J. Cozzi, Y. Li, Targeting PI3K/Akt/mTOR signaling pathway in the treatment of prostate cancer radioresistance. *Critical reviews in oncology/hematology* (2015) 96:507–517. doi: 10.1016/j.critrevonc.2015.07.005.
21. T. Gutschner, M. Hämmerle, M. Eißmann, J. Hsu, Y. Kim, G. Hung, A. Revenko, G. Arun, M. Stentrup, M. Groß, The noncoding RNA MALAT1 is a critical regulator of the metastasis phenotype of lung cancer cells. *Cancer research* (2013) 73:1180–1189. doi: 10.1158/0008-5472.CAN-12-2850.
22. Y. Fan, B. Shen, M. Tan, X. Mu, Y. Qin, F. Zhang, Y. Liu, TGF- $\beta$ -induced upregulation of malat1 promotes bladder cancer metastasis by associating with suz12. *Clinical cancer research* (2014) 20:1531–1541. doi: 10.1158/1078-0432.CCR-13-1455..
23. J.-H. Liu, G. Chen, Y.-W. Dang, C.-J. Li, D.-Z. Luo, Expression and prognostic significance of lncRNA MALAT1 in pancreatic cancer tissues. *Asian Pacific Journal of Cancer Prevention* (2014) 15:2971–2977. doi: 10.7314/apjcp.2014.15.7.2971.
24. L. Yang, H. Bai, Y. Deng, L. Fan, High MALAT1 expression predicts a poor prognosis of cervical cancer and promotes cancer cell growth and invasion. *Eur Rev Med Pharmacol Sci* (2015) 19:3187–3193.
25. J. Wang, L. Su, X. Chen, P. Li, Q. Cai, B. Yu, B. Liu, W. Wu, Z. Zhu, MALAT1 promotes cell proliferation in gastric cancer by recruiting SF2/ASF. *Biomedicine Pharmacotherapy* (2014) 68:557–564. doi: 10.1016/j.biopha.2014.04.007.
26. K. Liao, Y. Lin, W. Gao, Z. Xiao, R. Medina, P. Dmitriev, J. Cui, Z. Zhuang, X. Zhao, Y. Qiu, Blocking lncRNA MALAT1/miR-199a/ZHX1 axis inhibits glioblastoma proliferation and progression. *Molecular Therapy-Nucleic Acids* (2019) 18:388–399. doi: 10.1016/j.omtn.2019.09.005.
27. Y. Li, Z. Wu, J. Yuan, L. Sun, L. Lin, N. Huang, J. Bin, Y. Liao, W. Liao, Long non-coding RNA MALAT1 promotes gastric cancer tumorigenicity and metastasis by regulating vasculogenic mimicry and angiogenesis. *Cancer letters* (2017) 395:31–44. doi: 10.1016/j.canlet.2017.02.035.
28. H. YiRen, Y. YingCong, Y. Sunwu, L. Keqin, T. Xiaochun, C. Senrui, C. Ende, L. XiZhou, C. Yanfan, Long noncoding RNA MALAT1 regulates autophagy associated chemoresistance via miR-23b-3p sequestration in gastric cancer. *Molecular cancer* 16:1–12. doi: 10.1186/s12943-017-0743-3..
29. W. Chen, W. Zhao, L. Zhang, L. Wang, J. Wang, Z. Wan, Y. Hong, L.J.O. Yu, MALAT1-miR-101-SOX9 feedback loop modulates the chemo-resistance of lung cancer cell to DDP via Wnt signaling pathway. (2017) 8:94317.
30. H. Shaath, R. Vishnubalaji, R. Elango, S. Khattak, N.M. Alajez, Single-cell long noncoding RNA (lncRNA) transcriptome implicates MALAT1 in triple-negative breast cancer (TNBC) resistance to neoadjuvant chemotherapy. *Cell Death Discovery* (2021) 7:1–14. doi: 10.1038/s41420-020-00383-y..
31. C. Yuan, D. Wang, N. Zhang, Z. Wang, F. Yang, J. He, R. Sun, X. Yang, J. Hu, M. Wu, DNA damage/cGAS-triggered up-regulation of MALAT1 promotes undesirable inflammatory responses in radiotherapy of cancer. *Biochemical Biophysical Research Communications* 528:746–752. doi: 10.1016/j.bbrc.2020.05.064.
32. J. Guo, Y. Ding, H. Yang, H. Guo, X. Zhou, X. Chen, Aberrant expression of lncRNA MALAT1 modulates radioresistance in colorectal cancer in vitro via miR-101-3p sponging. *Experimental molecular*

- pathology (2020) 115:104448. doi: 10.1016/j.yexmp.2020.104448.
33. S. Sallé-Lefort, S. Miard, M.-A. Nolin, L. Boivin, M.-È. Paré, R. Debigaré, F. Picard, Hypoxia upregulates Malat1 expression through a CaMKK/AMPK/HIF-1 $\alpha$  axis. *International journal of oncology* (2016) 49:1731–1736. doi: 10.3892/ijo.2016.3630.
34. C. Li, Y. Cui, L.-F. Liu, W.-B. Ren, Q.-Q. Li, X. Zhou, Y.-L. Li, Y. Li, X.-Y. Bai, X.-B. Zu, High expression of long noncoding RNA MALAT1 indicates a poor prognosis and promotes clinical progression and metastasis in bladder cancer. *Clinical genitourinary cancer* (2017) 15:570–576. doi: 10.1016/j.clgc.2017.05.001.
35. K.-x. Ma, H.-j. Wang, X.-r. Li, T. Li, G. Su, P. Yang, J.-w. Wu, Long noncoding RNA MALAT1 associates with the malignant status and poor prognosis in glioma. *Tumor Biology* (2015) 36:3355–3359. doi: 10.1007/s13277-014-2969-7.
36. Y. Dong, G. Liang, B. Yuan, C. Yang, R. Gao, X. Zhou, MALAT1 promotes the proliferation and metastasis of osteosarcoma cells by activating the PI3K/Akt pathway. *Tumor Biology* (2015) 36:1477–1486. doi: 10.1007/s13277-014-2631-4..
37. X.-S. Wu, X.-A. Wang, W.-G. Wu, Y.-P. Hu, M.-L. Li, Q. Ding, H. Weng, Y.-J. Shu, T.-Y. Liu, L. Jiang, MALAT1 promotes the proliferation and metastasis of gallbladder cancer cells by activating the ERK/MAPK pathway. *Cancer biology therapy* (2014) 15:806–814. doi: 10.4161/cbt.28584.
38. P.L. Olive, J.P. Banáth, Phosphorylation of histone H2AX as a measure of radiosensitivity. *International journal of radiation oncology, biology, physics* (2004) 58:331–335. doi: 10.1016/j.ijrobp.2003.09.028.
39. C. Gong, Z. Yang, L. Zhang, Y. Wang, W. Gong, Y. Liu, therapy, Quercetin suppresses DNA double-strand break repair and enhances the radiosensitivity of human ovarian cancer cells via p53-dependent endoplasmic reticulum stress pathway. *OncoTargets* (2018) 11:17. doi: 10.2147/OTT.S147316..
40. M. Fernet, F. Mégnin-Chanet, J. Hall, V. Favaudon, Control of the G2/M checkpoints after exposure to low doses of ionising radiation: implications for hyper-radiosensitivity. *DNA repair* (2010) 9:48–57. doi: 10.1016/j.dnarep.2009.10.006..
41. S.-x. Zhang, Q.-h. Qiu, W.-b. Chen, C.-h. Liang, B. Huang, Celecoxib enhances radiosensitivity via induction of G2-M phase arrest and apoptosis in nasopharyngeal carcinoma. *Cellular Physiology Biochemistry* 33:1484–1497. doi: 10.1159/000358713.
42. P. Yao, Y. Li, W. Shen, X. Xu, Z. Wei, ANKHD1 silencing suppresses the proliferation, migration and invasion of CRC cells by inhibiting YAP1-induced activation of EMT. *American Journal of Cancer Research* 8:2311–2324.
43. S. Morla, Glycosaminoglycans and glycosaminoglycan mimetics in cancer and inflammation. *International journal of molecular sciences* (2019) 20:1963. doi: 10.3390/ijms20081963.
44. A. Salanti, T.M. Clausen, M.Ø. Agerbæk, N. Al Nakouzi, M. Dahlbäck, H.Z. Oo, S. Lee, T. Gustavsson, J.R. Rich, B. Hedberg, Targeting human cancer by a glycosaminoglycan binding malaria protein. *Cancer cell* (2015) 28:500–514. doi: 10.1016/j.ccell.2015.09.003.

45. N. Afratis, C. Gialeli, D. Nikitovic, T. Tsegenidis, E. Karousou, A.D. Theocharis, M.S. Pavão, G.N. Tzanakakis, N.K.J.T.F.j. Karamanos, Glycosaminoglycans: key players in cancer cell biology and treatment. (2012) 279:1177–1197. doi: 10.1111/j.1742-4658.2012.08529.x.

## Figures

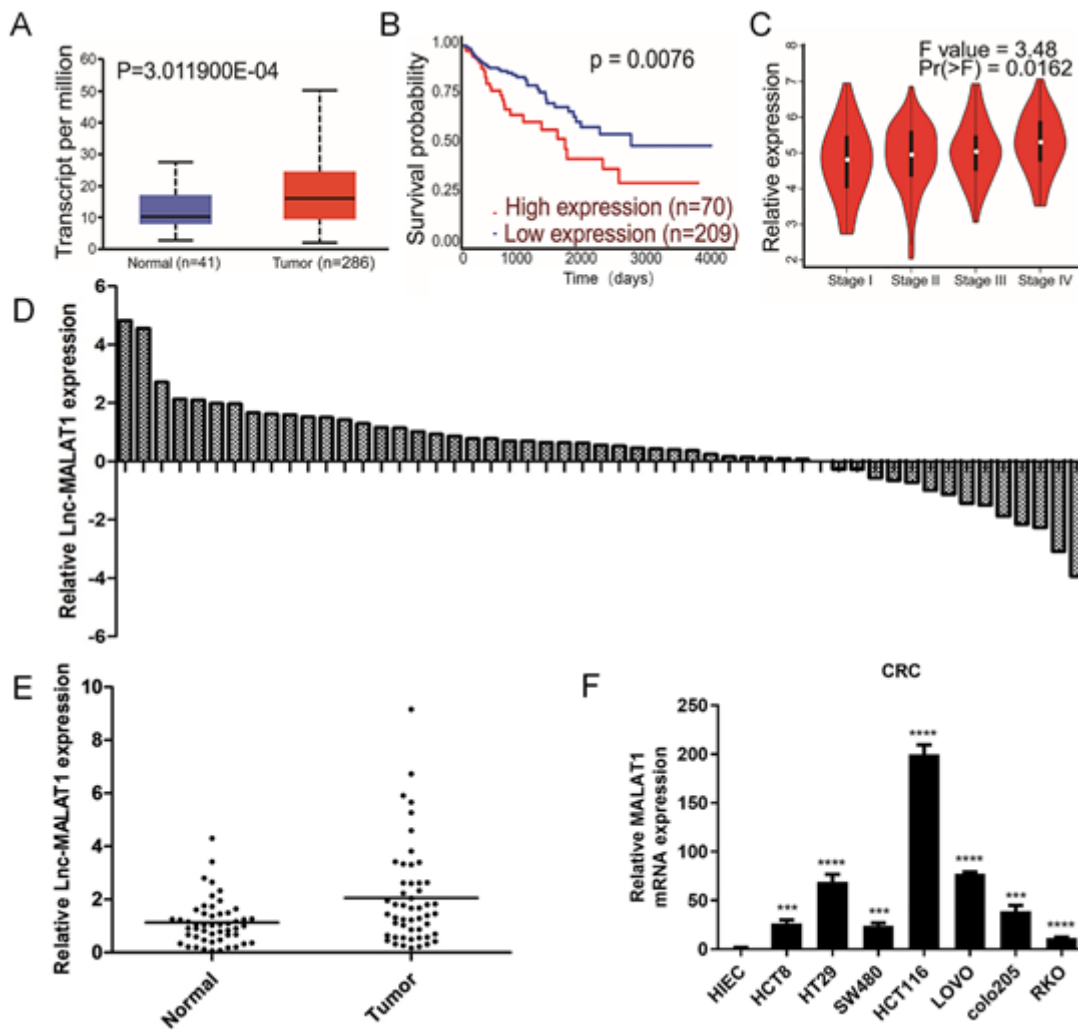


**Figure 1**

MALAT1 was related with tumor stage and survival, as well as upregulated in CRC tissues and cell lines. (A) MALAT1 mRNA levels in cancer tissues (red box) was high in normal (blue box). Results were assessed from TCGA cancer provisional data sets on the basis of TCGA Research Network (<http://cancergenome.nih.gov>). (B) Kaplan–Meier overall survival analysis of colorectal cancer patients from TCGA. P value was calculated using log-rank test. Relative expression of MALAT1 in different tumor stage. (C) MALAT1 mRNA levels in different tumor stage of human colorectal cancer tissues based on TCGA. (D) The distribution of MALAT1 expression of CRC tissues in every patient compared with that of its adjuvant normal tissues. (E) The comparison of MALAT1 expression in CRC tissues and adjuvant normal tissues. (F) The MALAT1 expression in normal cell line and CRC cell lines and. \*\*\*\*,  $p < 0.0001$ .

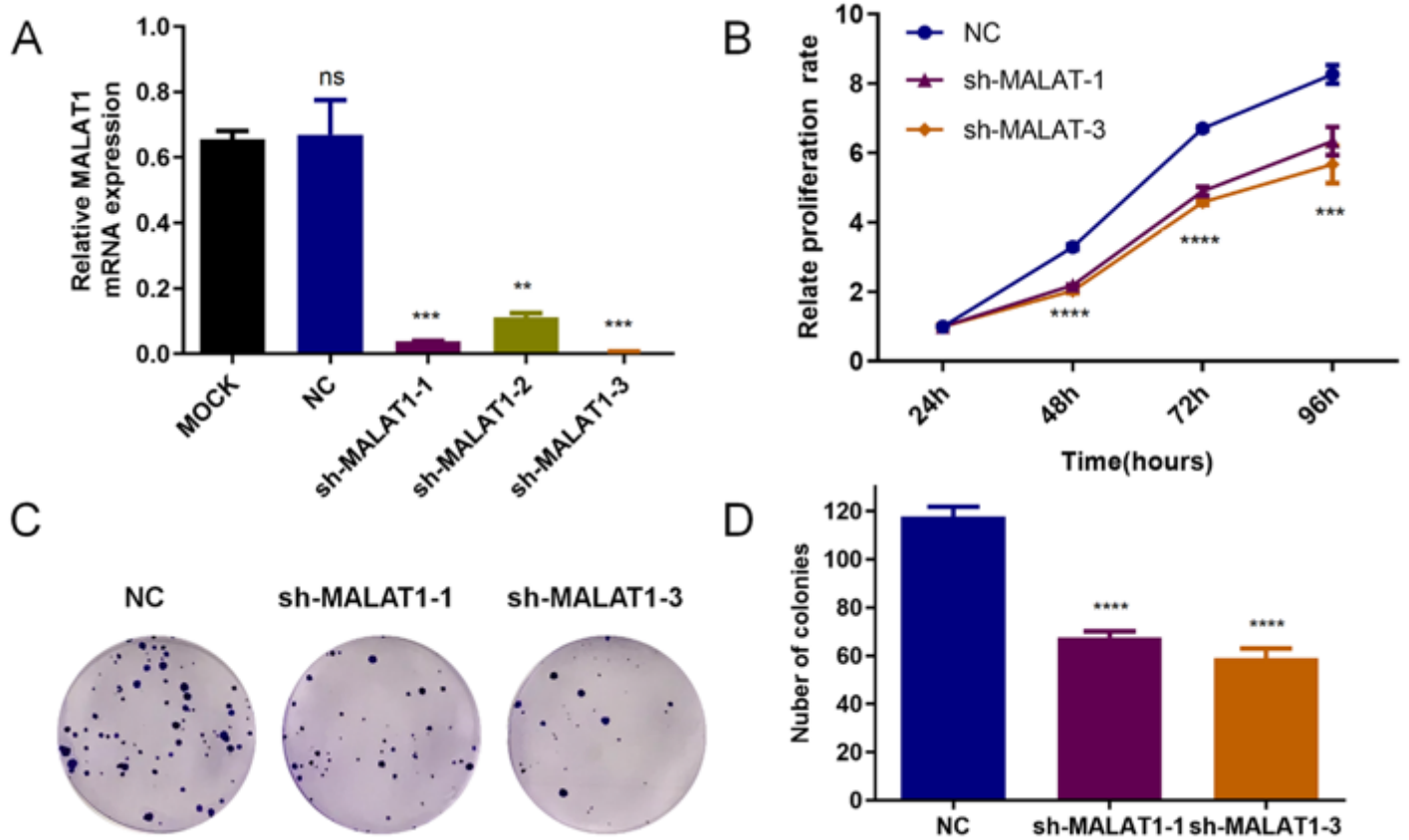


**Figure 2**

MALAT1 silencing inhibited proliferation of HCT 116 cell. (A) RT-PCR detecting the efficient transfection of shRNA target MALAT1 (\*\* $P < 0.001$ ). (B) Cells stably transfected were incubated for 24, 48, 72 and 96 h, and cell viability was detected by the CCK8 assay. (C) 200 cells were seeded into 6-well plates and cultured for 12–14 d. Colony formation containing at least 50 cells was counted. (D) Quantitative analysis of the colony numbers of HCT116 cells after transfecting with shRNA target MALAT1. The values are the mean  $\pm$  SD from three independent experiments. NC, negative control; \*\*\*\*,  $p < 0.0001$ .

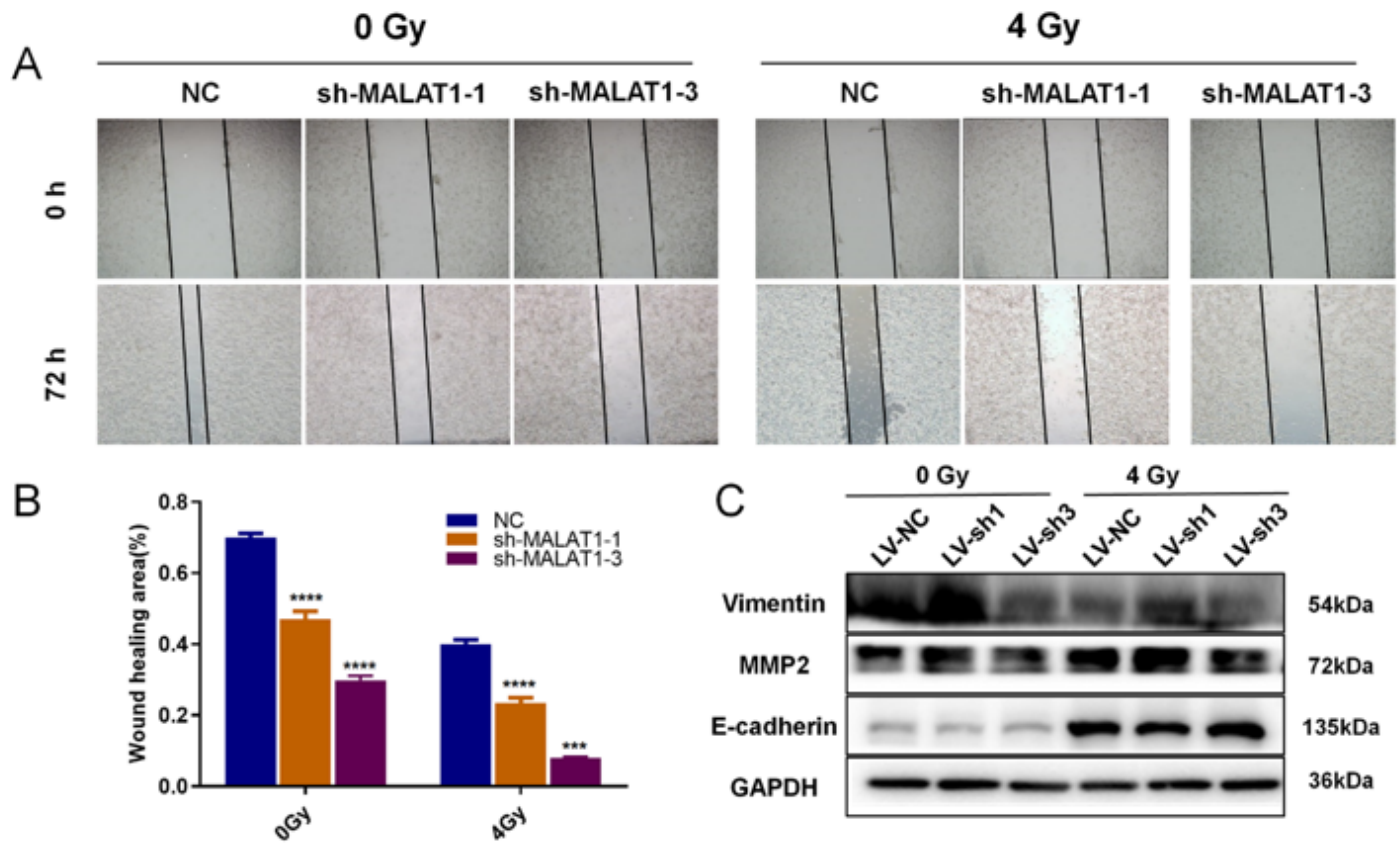


**Figure 3**

Knock down of MALAT1 plus radiotherapy impaired HCT116 migration. (A-B) MALAT1 silencing inhibited the ability of migration no matter combining with irradiation. (C) Expression of MMP2, E-cadherin and Vimentin was detected via western blot in combination of irradiation and MALAT1 silencing. \*\*\*,  $p < 0.001$ , \*\*\*\*,  $p < 0.0001$ . Full-length blots/gels are presented in Supplementary Figure 1A.

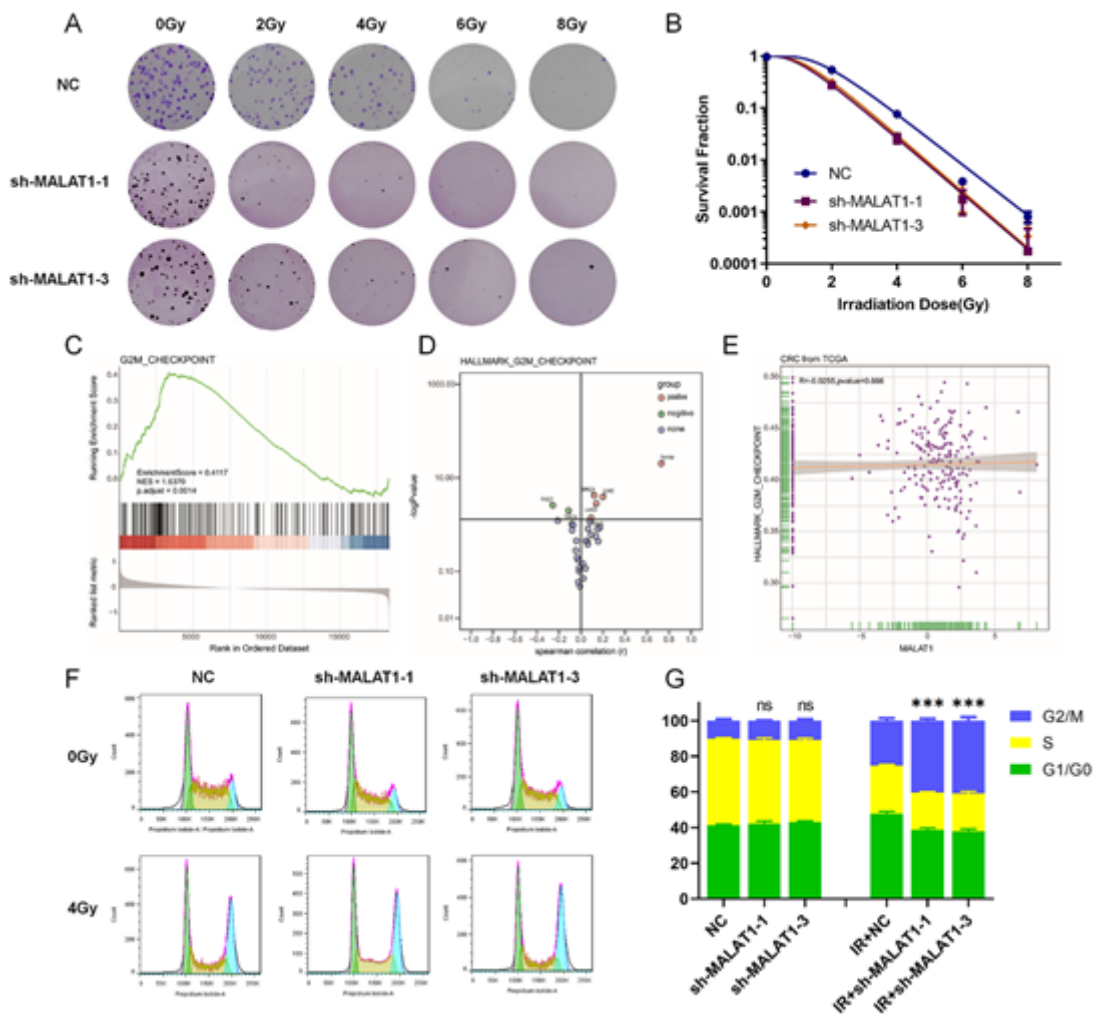


**Figure 4**

MALAT1 silencing increases the radiosensitivity of HCT116 cells. (A) MALAT1 silencing can increase the radiosensitivity of HCT116 cells. (B) Colony survival fraction at dose (0, 2, 4, 6 and 8 Gy) dependent manner compared to NC group. (C) GSEA of colorectal cancer expression profile in TCGA showed that G2M\_CHECKPOINT was upregulated. (D) Activation or inhibition of G2M\_CHECKPOINT pathway in 33 cancers. (E) Correlation analysis of MALAT1 expression level and G2M\_CHECKPOINT in colorectal cancer. (F&G) MALAT1 silencing combined with radiation results in more HCT116 cells entering G2/M-phase arrest at 12 h. \*\*\*\*,  $p < 0.001$

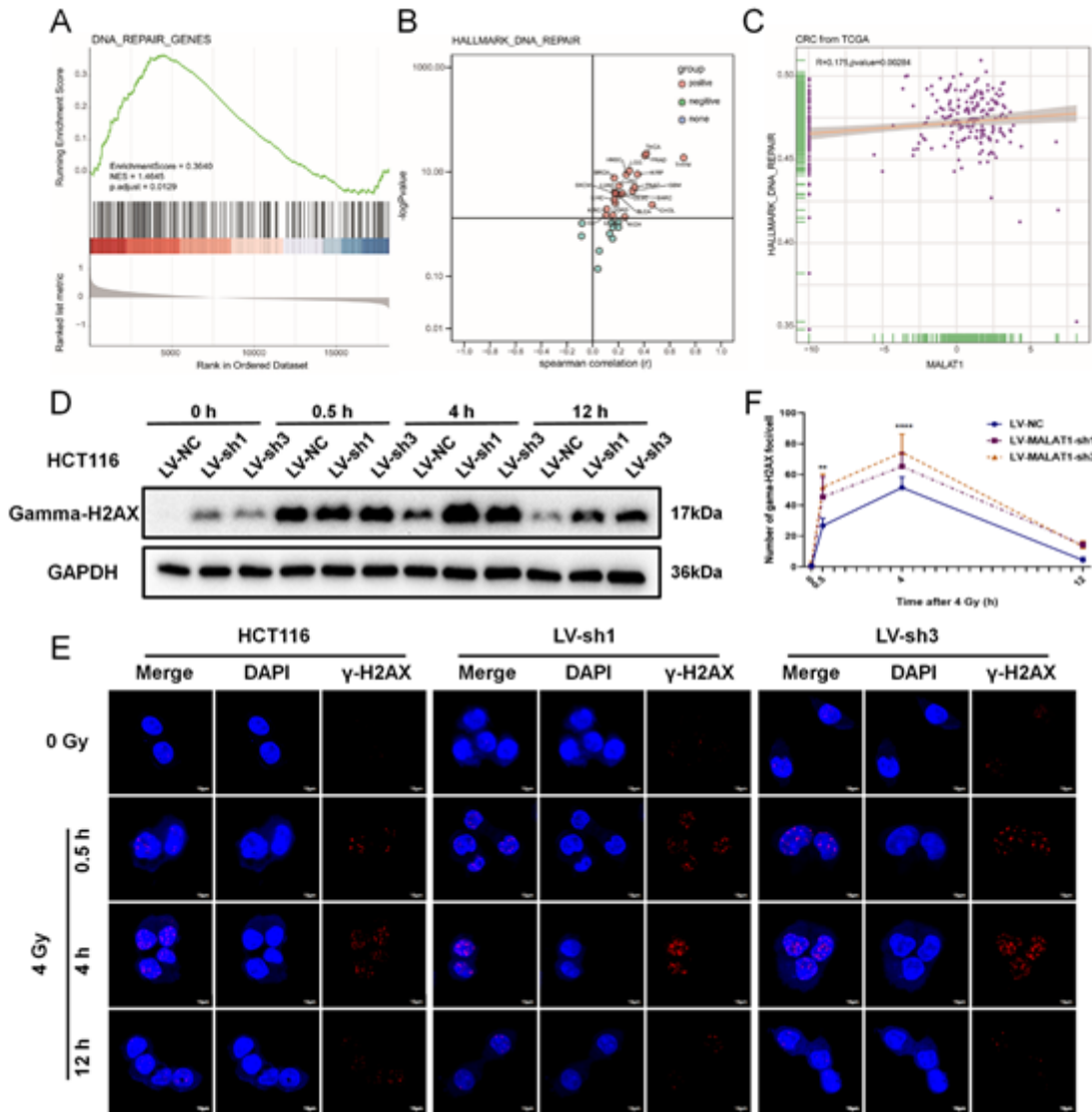


**Figure 5**

MALAT1 silencing induced DNA double-strand breaks in HCT116. (A) GSEA of colorectal cancer expression matrix in TCGA showed that DNA\_REPAIR was upregulated. (B) Activation or inhibition of DNA\_REPAIR in 33 cancers. (C) Correlation analysis of MALAT1 expression level and DNA\_REPAIR in CRC. (D) Downregulation of MALAT1 increase the expression level of  $\gamma$ -H2AX protein induced by irradiation at 0, 0.5, 4, and 12 h in HCT116. (E&F) The formation of nuclei  $\gamma$ -H2AX foci was further confirmed by immunofluorescence. \*\*,  $p < 0.01$ , \*\*\*,  $p < 0.001$ , \*\*\*\*,  $p < 0.0001$ . Full-length blots/gels are presented in Supplementary Figure 1B.

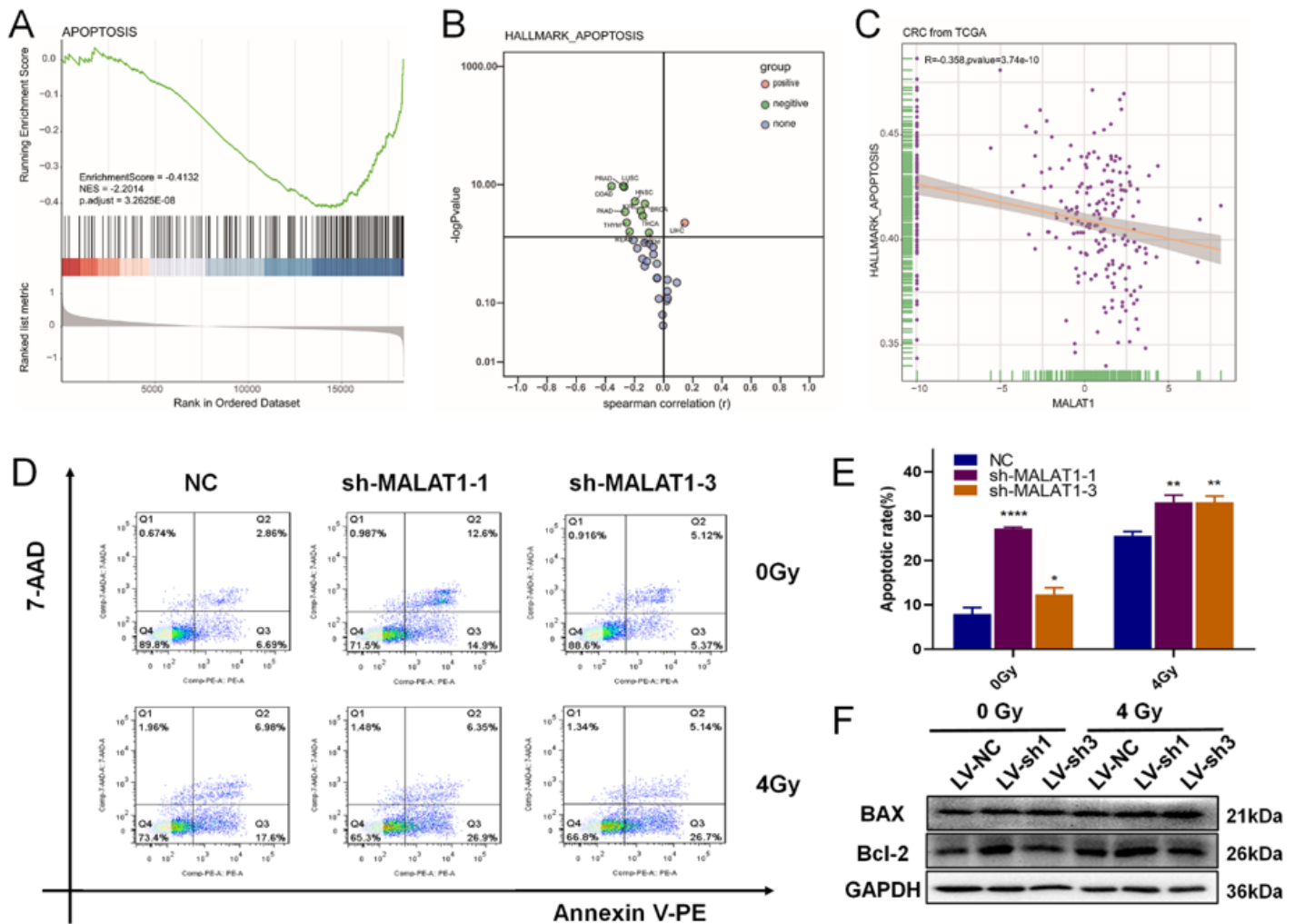


**Figure 6**

MALAT1 silencing induced apoptosis in HCT116. (A) GSEA of colorectal cancer expression matrix in TCGA indicated that APOPTOSIS was downregulated. (B) Apoptotic pathway status in 33 cancers. (C) Correlation analysis of MALAT1 and APOPTOSIS in CRC. (D) MALAT1 silencing increased the apoptosis level in HCT116 induced by irradiation after 48 h. (E) The apoptosis rate of every group was statistics by FlowJo. (F) Western blot showed the expression of apoptosis-related proteins in the combination treatments of shRNA MALAT1 and radiation. \*\*,  $p < 0.01$ , \*\*\*,  $p < 0.001$ , \*\*\*\*,  $p < 0.0001$ . Full-length blots/gels are presented in Supplementary Figure 1C.

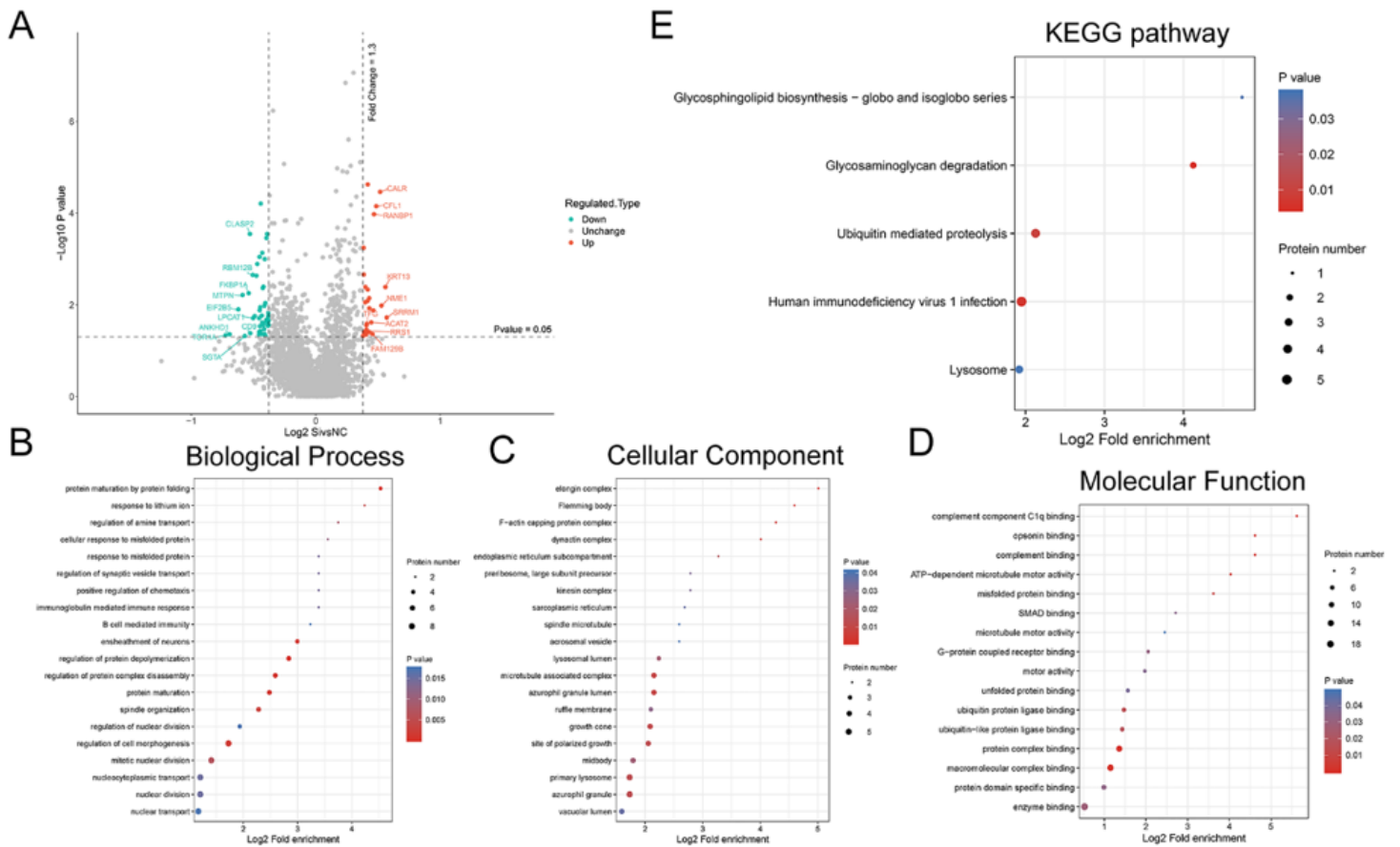


**Figure 7**

iTRAQ proteomic analysis of HCT116 siMALAT1 compared with siNC. (A) Volcano plot of the top 10 up and down-regulated proteins. (B) Biological Process was mainly enriched in ‘protein maturation by protein folding’, ‘regulation of protein depolymerization’, ‘regulation of protein complex disassembly’, ‘ensheathment of neurons’, and ‘protein maturation’. (C) Cellular Component was mainly enriched in ‘elongin complex’, ‘Flemming body’, ‘F-actin capping protein complex’, ‘dyactin complex’, and ‘microtubule associated complex’. (D) Molecular Function analysis implied that most of regulated genes were enriched in ‘complement component C1q binding’, ‘protein complex binding’, ‘macromolecular complex binding’, ‘complement binding’, and ‘opsonin binding’. (E) KEGG pathway analysis showed that glycosaminoglycan degradation, Human immunodeficiency virus 1 infection, Ubiquitin mediated proteolysis, Glycosphingolipid biosynthesis - globo and isoglobo series, Lysosome, pathways were mainly enriched. The larger the bubble represented the more DAPs. P-value was displayed in the color of the bubble, and small p-value denoted greater significance.

## Supplementary Files

This is a list of supplementary files associated with this preprint. Click to download.

- [SupplementalTable4.xlsx](#)

- [SupplementalTable5.xlsx](#)
- [SupplementalTable6.xlsx](#)
- [SupplementalTable7.xlsx](#)
- [SupplementalTable8.xlsx](#)
- [SupplementalTable9.xlsx](#)
- [Supplementarydata.docx](#)